

Petrology of a new basaltic shergottite: Dhofar 378

Yukio Ikeda^{1*}, Makoto Kimura¹, Hiroshi Takeda², Gen Shimoda³, Noriko T. Kita³,
Yuichi Morishita³, Akio Suzuki⁴, Emil Jagoutz⁵ and Gerlind Dreibus⁵

¹*Department of Material and Biological Science, Ibaraki University, Mito 310-8512*

²*Research Institute, Chiba Institute of Technology, Narashino 275-0016*

³*National Institute of Advanced Industrial Science and Technology, Tsukuba 305-8567*

⁴*Faculty of Science, Tohoku University, Sendai 980-8578*

⁵*Max-Planck-Institute für Chemie, P.O. Box 3060, D-55020 Mainz, Germany*

**Corresponding author. E-mail: y-ikeda@mx.ibaraki.ac.jp*

(Received October 4, 2005; Accepted August 15, 2006)

Abstract: Dhofar 378 is a new basaltic shergottite, consisting mainly of pyroxenes, plagioclase glass, phosphates, titanomagnetite, and mesostasis. It is one of the most ferroan shergottites and resembles the Los Angeles shergottite. Pyroxenes show remarkable chemical zoning from 0.4 of Mg/(Mg + Fe) to less than 0.1, and their REE patterns are depleted in light REE whereas the REE pattern of the bulk Dhofar 378 is flat. All plagioclase grains in the original lithology completely melted by an intense impact shock, and the plagioclase melts crystallized fibrous plagioclase to form the rims surrounding the plagioclase melts. Then, the melts quenched as plagioclase glass to form the cores. The shock stage of Dhofar 378 is higher than that of the Los Angeles shergottite. The degree of impact shock for Dhofar 378 may be about 55–75 GPa and is the highest among all known martian meteorites.

key words: martian meteorites, basaltic shergottites, plagioclase glass, differentiated magmas, intense impact shock

1. Introduction

The new basaltic shergottite Dhofar 378 was recovered from the Oman desert. The total mass recovered is 15 g with fresh fusion crust. It was approved as a shergottite by the Nomenclature Committee of the Meteoritical Society in December 2001 (Russell *et al.*, 2002). Its lithology is doleritic (or diabasic) with a subophitic texture, and the grain sizes of the main phases (plagioclase glass and pyroxenes) are 1 to a few mm in length (Fig. 1c). Therefore, Dhofar 378 is an olivine-free dolerite type (Ikeda, 2004), which is similar to Shergotty, Zagami, EETA79001B, Los Angeles and so on. However, it is not a typical dolerite type; the hand specimens contain many bubble-like pores, all plagioclase grains have changed to plagioclase glass, and the plagioclase glass sometimes shows a flow structure. In addition, the pyroxenes in Dhofar 378 are more ferroan than other shergottites. Dhofar 378 differs in the appearance and the compositions from other basaltic shergottites. Therefore, the detailed study of Dhofar 378 may give us important clues to clarify the differentiation

processes of martian magmas. In this paper, detailed petrology and mineralogy are presented, and the major element bulk chemistry and geochemical data including REE patterns are also discussed.

2. Analytical method

Three thin sections (α , β , γ) of Dhofar 378 were prepared from a 1.24 g chip for this petrological and mineralogical study. Chemical compositions of the constituent minerals were obtained using an electron-probe microanalyzer (EPMA; JEOL 733 at Ibaraki Univ.). A sample current of 5–10 nA, accelerating voltage of 15 kV, and measuring time of 10 s for a peak and background were adopted. The corrections were carried out by the Bence and Albee method for silicates and oxides (Bence and Albee, 1968), and the standard ZAF method for sulfides.

The major element bulk composition of Dhofar 378 was obtained by an X-ray fluorescence (Rigaku, system 3270E at Ibaraki Univ.) method using a glass bead, which was made by heating of a powder sample mixed the Dhofar 378 powder with a flux powder of lithium meta-borate. The Dhofar 378 powder was made from a few pieces of 550 mg, the mixing ratio of the flux and the Dhofar 378 sample was 20:1, and the heating time was 5 min to produce the glass beads. The standard materials of JB-1 (Basalt, The Geological Survey of Japan), JB-3, JA-1 (Andesite), JP-1 (Peridotite), JGB (Gabbro), and JB-1 added with minor oxide reagents of Fe, Cr, Mn, and P were used for the calibration curve. The standard deviation was calculated from chemical compositional range of a Dhofar 378 glass bead sample obtained by 20 times multiple measurements. The bulk composition of Dhofar 378 was also obtained by the instrumental activation analysis (Dreibus *et al.*, 2002), using a 97 mg sample.

The modal composition of Dhofar 378 was obtained by measuring the point percents of the constituent phases using a focused beam of EPMA. The total number of points was 3000 for a thin section (α). Raman spectra of some constituent phases were measured to identify the phases by a spectrometer at Tohoku University (JASCO NRS-2000 with a nitrogen-cooled CCD detector). A microscope was used to focus the excitation laser beam (514.5 nm lines of a Princeton Instruments Inc. Ar+laser) to a 2 μ m spot. The laser power was 40 mW.

REE contents of pyroxenes were measured by a secondary ion mass spectrometry (SIMS, Cameca IMS-1270) of National Institute of Advanced Industrial Science and Technology. The analytical method is shown in Togashi *et al.* (2003) and Kita *et al.* (2004).

3. Petrography and modal composition

Dhofar 378 contains many bubble-like pores ranging from 0.1 mm to a few mm in diameter, which may have formed by an intense impact shock (Fig. 1a). The cut surface shows a texture consisting of whitish and darkish phases, and the boundaries between the two are diffuse and unclear (Fig. 1b). Thin sections of Dhofar 378 show a flow structure of plagioclase glass (Pl-glass) (Fig. 1c), which suggests that the plagioclase grains in Dhofar 378 were once molten.

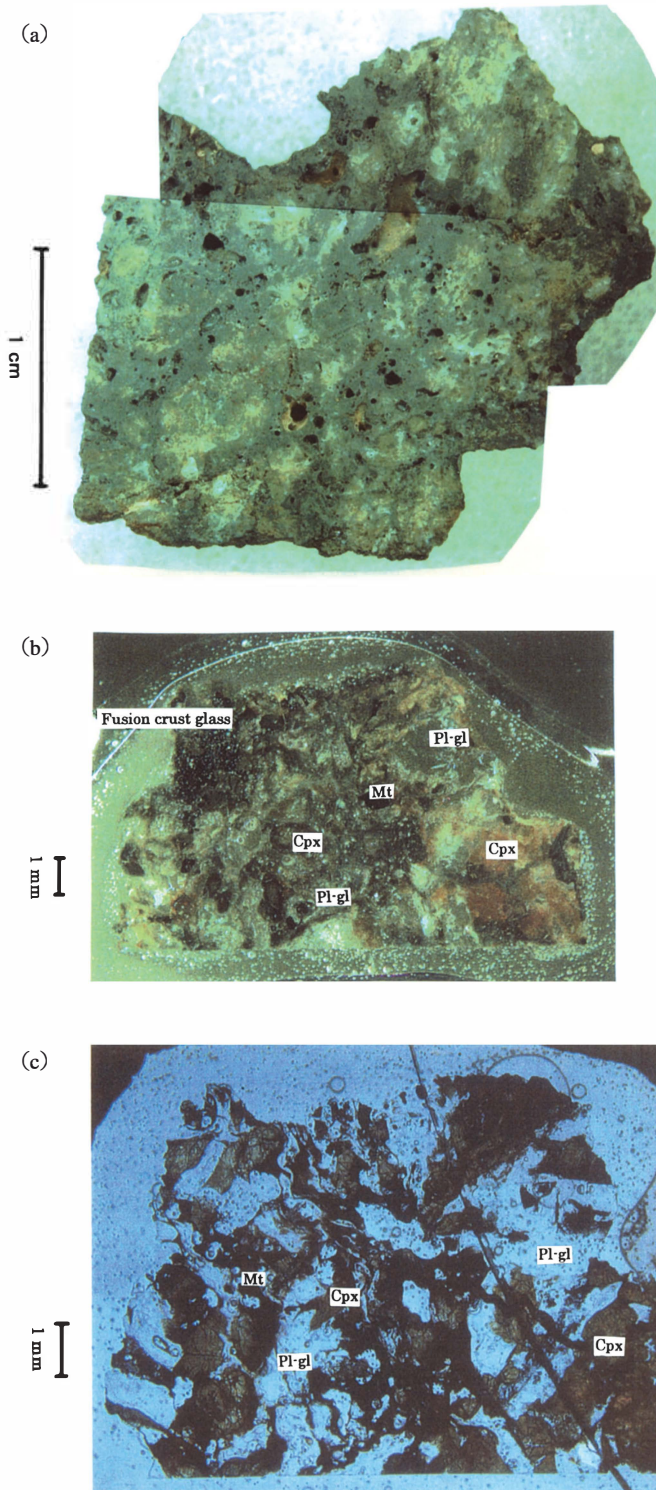


Fig. 1. Photomicrographs of the Dhofar 378 basaltic shergottite. (a) A chip under a microscope. (b) A thick section of Dhofar 378 under a microscope. (c) A thin section under a petrological microscope with an open Nicol. Abbreviations: plagioclase glass (Pl-gf), titanomagnetite (Mt), and clinopyroxene (Cpx).

Dhofar 378 is a basaltic shergottite, and the main phases are clinopyroxene (augite and pigeonite), Pl-glass, Ti-rich magnetite and Ca-phosphates. The Pl-glass often shows relict outlines of phenocrystic plagioclase, and the long dimensions are 1 to a few mm. It always has a plagioclase rim which is never broken, suggesting that it crystallized after the flow of plagioclase melt. The clinopyroxenes are also phenocrystic, and sometimes partly include phenocrystic Pl-glass, resulting in the subophitic texture. Titanomagnetite grains always contain exsolution lamellae of ilmenite, and the host-lamellae ratio is about 9:1. Ca-phosphates are whitlockite and apatite in a rough ratio of 4:1. There occurs mesostasis among the main phases. The mesostasis contains alkali feldspar, silica phases (quartz and silica glass), K-rich (rhyolitic or milky) glass, and Ca-phosphates. The other minor phases are hedenbergite, pyroxferroite, fayalite, and sulfide (pyrrhotite). Shock-melt veins are common in Dhofar 378, consisting mainly of clinopyroxene and/or plagioclase. They sometimes cut through pyroxene grains and Pl-glass grains. Calcite occurs as a terrestrial weathering product. The modal composition of the stone is shown in Table 1 with that of the Los Angeles shergottite, which is very similar in mineral assemblages and compositions to Dhofar 378, although the MgO content of Dhofar 378 is more than that of Los Angeles. Dhofar 378 is richer in clinopyroxenes and poorer in mesostasis than the Los Angeles shergottite.

4. Pairing

Dhofar 378 was found near the area where the Dhofar 019 olivine-phyric shergottite was recovered. The latter is doleritic, but it contains olivine grains with Mg/

Table 1. Modal composition (vol%) for Dhofar 378 with reference to those for the Los Angeles shergottite.

	Dhofar 378	Los Angeles Rubin <i>et al.</i> (2000) LA1 and LA2	Los Angeles Mikouchi (2001)
Clinopyroxene	49.3%	40.7%, 37.7%	41.60%
Plagioclase glass	43.5%		0
Maskelynite	0	47.9%, 43.6%	45%
Ti-rich Magnetite (Mt) with Ilmenite (Ilm)	2.0% (Mt 1.8%, Ilm 0.2%)	2.3%, 3.7% (Ulvösp+Ilm)	1.70%
Phosphates	1.4% (Whit 1.1%, Ap 0.3%)	1.8%, 2.7%	2.30%
Mesostasis	3.2% (K-rich glass 1.8%, Silica 1.1%, Fa,Hd,Pxf 0.3%)	6.7%, 11.5% (Silica+Fa+K-rich glass)	9.40%
Pyrrhotite	0.6%	0.5%, 0.7%	

Abbreviation: whitlockite (Whit), apatite (Ap), a silica mineral and silica glass (Silica), fayalite (Fa), hedenbergite (Hd), magnetite (Mt), ilmenite (Ilm), ulvöspinel (Ulvösp) and pyroxferroite (Pxf). Plagioclase glass includes plagioclase rims surrounding Pl-glass cores, and K-rich glass contains K-feldspar.

(Mg + Fe) atomic ratios (hereafter, mg#) of 0.60–0.25 (Grossman, 2001). Dhofar 378 does not contain magnesian olivines. In addition, pyroxenes in Dhofar 019 are more magnesian than those in Dhofar 378. Therefore, Dhofar 019 is not a pair with Dhofar 378. Dhofar 378 is rather similar in lithology to the Northwest Africa 480 basaltic shergottite which has no magnesian olivine and a homogeneous maskelynite (An_{46-50}), but the latter has more magnesian pyroxenes than the former (Grossman, 2001). Dhofar 378 rather resembles the Los Angeles basaltic shergottite: Lithology, texture, grain size, mineral assemblage, and mineral compositions of the latter (Rubin *et al.*, 2000; Warren *et al.*, 2004) are nearly identical to those of the former. However, plagioclase grains in the Los Angeles shergottite have changed to maskelynite, although those in Dhofar 378 to Pl-glass, indicating that the degree of impact shock differs between the two. Dhofar 378 is not a pair with any other basaltic shergottites.

5. Bulk composition and fusion-crust glass

5.1. Bulk composition of major elements

The major element chemical composition of Dhofar 378 was obtained by the X-ray fluorescence method and the result is shown in Table 2. The chemical composition of Dhofar 378 was also obtained by the instrumental neutron activation analyses (INAA) at Mainz (Dreibus *et al.*, 2002), and it is also shown in Table 2. The chemical compositions of the two are different from each other. This difference may be a sampling problem; the fluorescence analyses used 550 mg, although the INAA used 97 mg. The fluorescence sample may contain more clinopyroxene grains, although the INAA sample may contain more plagioclase and phosphate components. Dhofar 378 is a coarse-grained rock consisting of major minerals with about 1 mm size, and thus we may need more than a few grams of the sample to obtain more accurate whole rock composition. Therefore, the weight-mean composition of the two bulks should be adopted for the bulk composition of Dhofar 378, and is shown in Table 2. The weight-mean bulk chemical composition of Dhofar 378 is very similar to that of the Los Angeles shergottite (Warren *et al.*, 2000), although the MgO content of the former is more than that of the latter. Their chemical and petrographical similarity suggests that their original rocks prior to the impact shock were similar; the original rocks of the two shergottites seem to have had the similar mineral assemblages, grain size, and textures to each other.

5.2. Fusion-crust glass

The fusion crust of Dhofar 378 consists mainly of black glass with many bubbles, the sizes of which are usually 10–100 μm in diameters. Chemical compositions of the black fusion-crust glass were obtained by EPMA, and the average composition is shown in Table 2. The black fusion-crust glass has a chemical composition similar to the bulk composition, but it seems to be slightly more depleted in plagioclase components than the bulk composition. The black fusion-clast glass was produced by melting and mixing of the Pl-glass and clinopyroxene with magnetite, phosphate and mesostasis components. As the viscosity of the plagioclase melt is high, the plagioclase component may not be completely mixed into the black fusion-crust glass, resulting in the slight depletion of plagioclase component. This idea is supported by the fact that Pl-glass

Table 2. The bulk compositions of the Dhofar 378 shergottite were obtained by the X-ray fluorescence analyses using a 550 mg sample (columns 2 and 3) and by the instrumental neutron activation analyses (INAA, Dreibus *et al.*, 2002) using a 97 mg sample (column 4). The weight mean composition (column 5) was calculated from the compositions obtained by the two methods. The chemical composition of the black fusion-crust glass (column 6) was obtained by EPMA analyses. The bulk composition of the Los Angeles shergottite (column 7; Warren *et al.*, 2000) is shown for reference.

	Bulk (550 mg) Fluorescence 2σ		Bulk (97 mg) INAA	Weight-mean Bulk	Fusion-crust glass Dhofar 378, EPMA	Bulk (LA2) Los Angeles
SiO ₂	49.88	0.101	49	49.75	48.08	48.5
TiO ₂	0.98	0.007	<i>1</i>	0.98	1.18	1.35
Al ₂ O ₃	10.08	0.066	15.8	10.94	9.5	10.55
Cr ₂ O ₃	0.04	0.002	0.038	0.04	0	0.014
FeO*	19.94	0.017	15.66	19.3	21.11	21.4
MnO	0.48	0.004	0.38	0.46	0.55	0.49
MgO	5.66	0.079		5.48**	5.35	3.73
CaO	10.32	0.011	10.45	10.34	9.76	9.9
Na ₂ O	1.98	0.069	2.64	2.08	2.31	2.17
K ₂ O	0.17	0.003	0.2	0.17	0.15	0.3
P ₂ O ₅	0.70	0.007	1.2	0.77	0.9	1.5
Total	100.23		96.368	100.31	98.89	99.904
mg#	0.336			0.336	0.311	0.237

σ : Standard deviation (σ) was obtained by the 20 time multiple measurement of a Dhofar 378 glass bead. The data of italic in column 4 are estimated ones (Dreibus *et al.*, 2002). FeO*: All iron as FeO. MgO** content of the mean was obtained from the MgO of the fluorescence value (5.66 wt%) under an assumption that mg# of the fluorescence value is the same as that of the mean.

patches are sometimes observed in the black fusion-crust glass, as an unmixed remnant component. The chemical composition of the fusion-crust glass in Dhofar 378 is also similar to those of the Los Angel shergottite (Warren *et al.*, 2000), supporting that the original rocks were similar to each other.

5.3. REE contents of pyroxenes and the bulk meteorite

The pyroxene phenocrysts in Dhofar 378 show normal zoning from augite cores to pigeonite rims (Fig. 2a). The core of a pyroxene grain in Fig. 2a is augite with mg# = 0.58, and the rim is pigeonite with mg# = 0.25. Rare earth element contents of the pyroxene cores and rims were measured using SIMS (Table 3). The CI-normalized REE patterns of the pyroxenes are shown in Fig. 3. Generally speaking, REE contents of pyroxene rims are higher by a factor of 2–10 than pyroxene cores for shergottites (Lundberg *et al.*, 1988; McSween *et al.*, 1996). Although the REE patterns of the pyroxenes in Dhofar 378 are similar to those of other basaltic shergottites, there is no difference in REE contents of pyroxenes for Dhofar 378 between the core and rim. This is because pyroxenes #1 and #2 are high-Ca pyroxenes with CaO = 14–15 wt%, although pyroxenes #3 and #4 are low-Ca pyroxene with CaO = 7–8 wt%. As REE

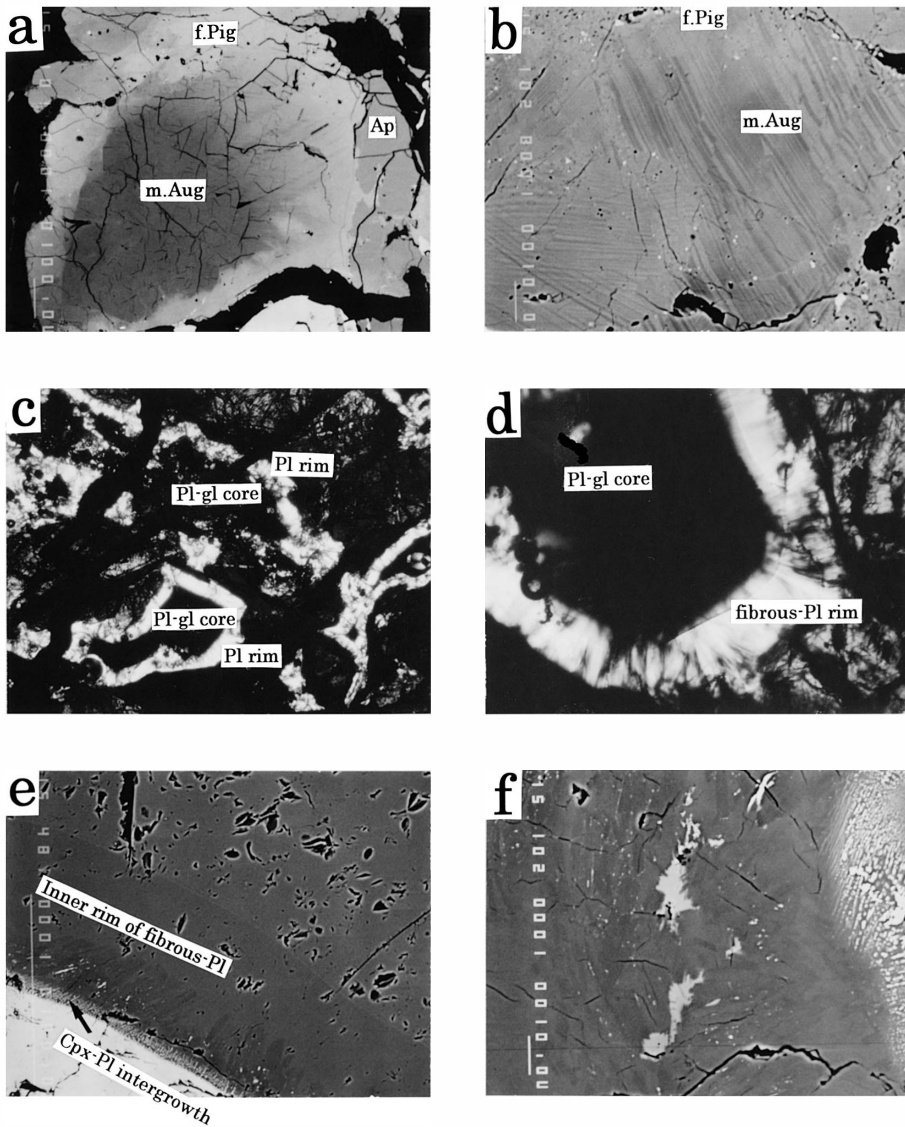


Fig. 2. Back scattered electron (BSE) images or optical microscope images of Dhofar 378. (a) A BSE image of a clinopyroxene with chemical zoning from augite core to pigeonite rim. Magnesian augite (m.Aug), ferroan pigeonite (f.Pig), and apatite (Ap). The width is about $1100\ \mu\text{m}$. (b) A BSE image of a clinopyroxene with exsolution lamellae. A darker phase is magnesian augite, and a brighter phase is ferroan pigeonite. The width is about $110\ \mu\text{m}$. (c) A core-rim texture of plagioclase glass grains with crossed Nicols under an optical microscope. Abbreviation: Plagioclase (Pl). The width is about $3.6\ \text{mm}$. (d) An enlarged image of the core-rim texture of a plagioclase glass grain with crossed Nicols under a microscope. Note fibrous plagioclase rim and Becke's line between core and rim. The width is about $740\ \mu\text{m}$. (e) A BSE image of inner and outer rims of a plagioclase grain. The outer rim consists of clinopyroxene-plagioclase intergrowth. The width is about $230\ \mu\text{m}$. (f) A BSE image of fibrous plagioclase (gray) and K-Fe-rich glass (white). The width is about $110\ \mu\text{m}$.

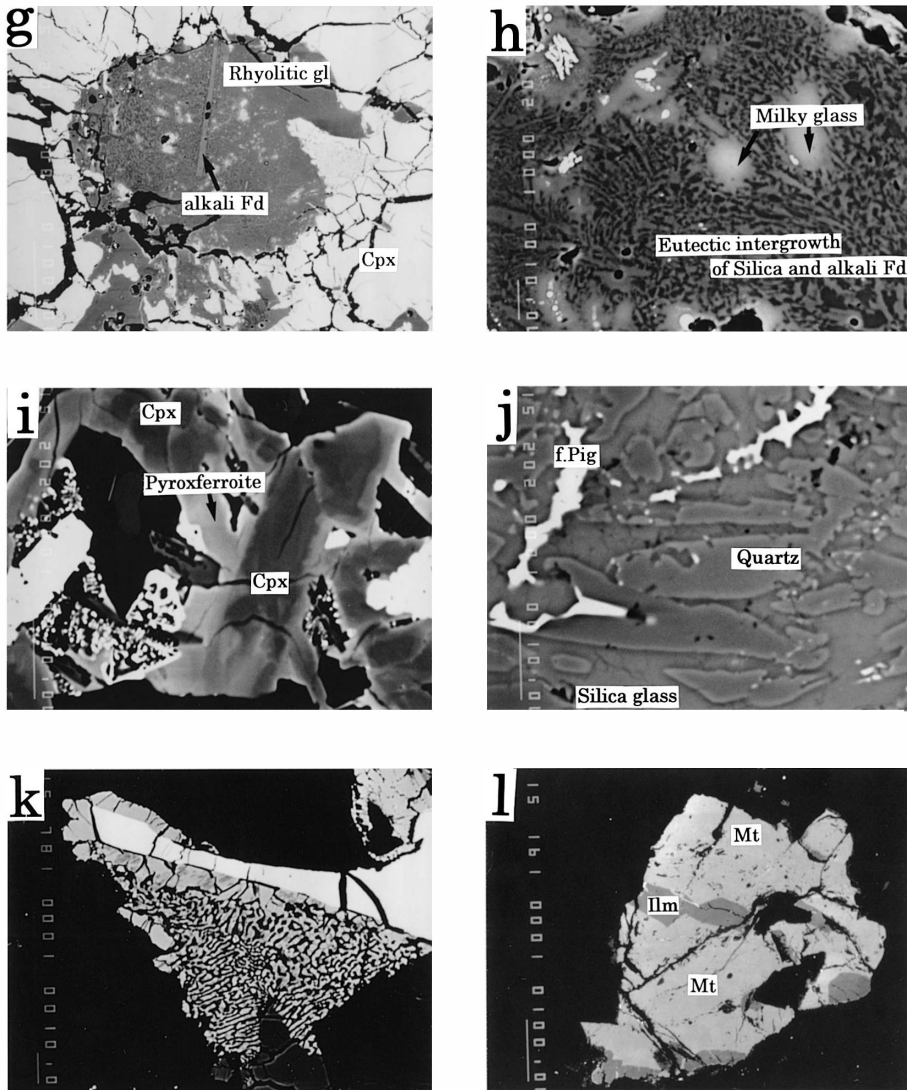


Fig. 2 (continued).

(g) A BSE image of rhyolitic glass and alkali feldspar (Fd). The width is about 540 μm . (h) A BSE image of milky glass and eutectic intergrowth. The width is about 110 μm . (i) A BSE image of Ti-rich augite (Cpx) and pyroxferroite in mesostasis. The width is about 54 μm . (j) A BSE image of quartz and silica glass. The width is about 540 μm . (k) A BSE image of intergrowth of fayalite and silica with minor clinopyroxene. The width is about 150 μm . (l) A BSE image of a titanomagnetite grain with ilmenite lamellae. The width is about 700 μm .

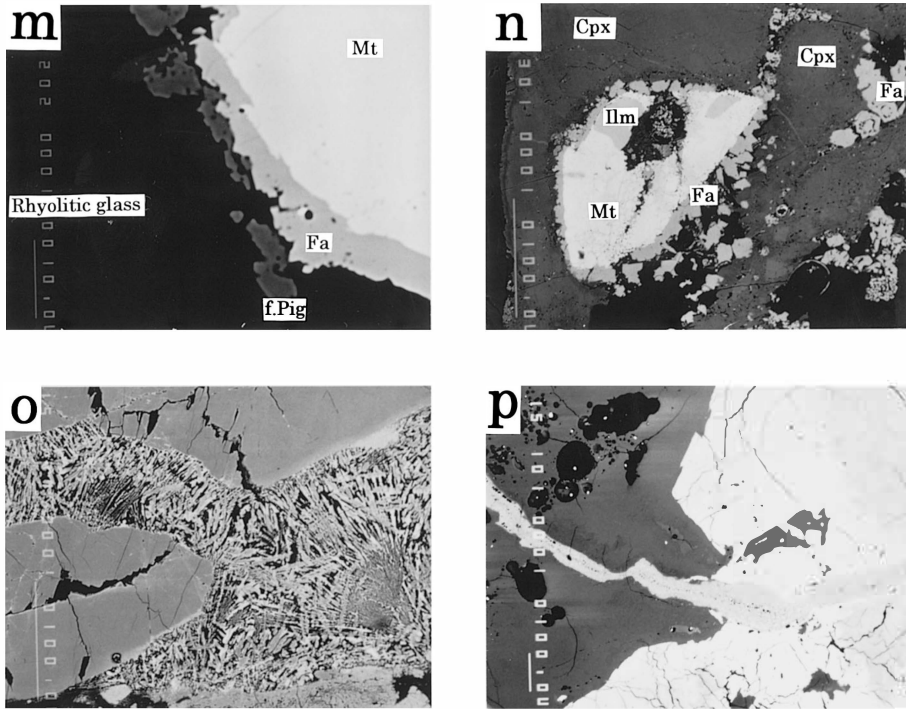


Fig. 2 (continued).

(m) A BSE image of fayalite grains between titanomagnetite and rhyolitic glass. The width is about $54\mu\text{m}$. (n) A BSE image of a titanomagnetite grain surrounded by fayalite grains. Fayalite (Fa), titanomagnetite (Mt), and ilmenite (Ilm). The width is about $370\mu\text{m}$. (o) A BSE image of a shock-melt vein consisting mainly of pyroxene. The width is about $360\mu\text{m}$. (p) A BSE image of a vein consisting mainly of pyroxene and plagioclase. The width is about $1250\mu\text{m}$.

Table 3. REE contents (in ppm) of a zoned pyroxene grain (augitic cores #1 & #2; pigeonitic rims #3 & #4) in Dhofar 378. Their CI-normalized contents are also shown.

	La	Ce	Pr	Nd	Sm	Eu	Gd	Tb	Dy	Ho	Er	Tm	Yb	Lu
Pyx #1	0.08	0.39	0.1	0.63	0.33	0.15	0.74	0.21	1.36	0.29	0.83	0.11	0.89	0.12
CI norm	0.3	0.63	1.1	1.3	2.2	2.6	3.6	5.6	5.3	5.2	5.0	4.4	5.2	4.7
Pyx #2	0.07	0.26	0.06	0.32	0.34	0.11	0.61	0.13	1.16	0.28	0.8	0.14	1.26	0.17
CI norm	0.3	0.43	0.6	0.68	2.2	1.8	3.0	3.4	4.6	4.9	4.9	5.6	7.4	6.7
Pyx #3	0.04	0.18	0.04	0.24	0.2	0.09	0.50	0.11	1.2	0.28	0.90	0.15	1.39	0.23
CI norm	0.2	0.30	0.4	0.51	1.3	1.5	2.4	2.9	4.7	4.9	5.5	5.9	8.2	8.9
Pyx #4	0.02	0.16	0.04	0.26	0.26	0.1	0.40	0.1	0.88	0.25	0.70	0.11	0.80	0.18
CI norm	0.1	0.26	0.4	0.56	1.7	1.8	1.9	2.7	3.5	4.4	4.2	4.2	4.7	7.1

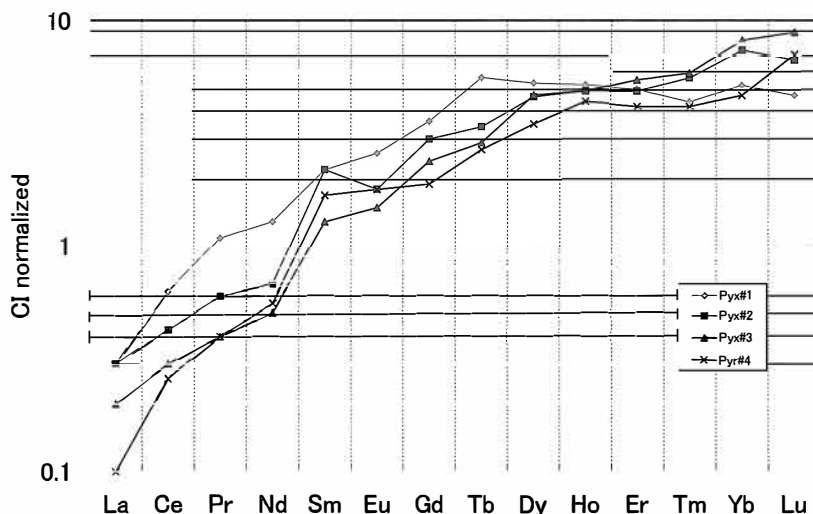


Fig. 3. Rare earth elements of pyroxene core (#1 & #2) and rim (#3 & #4) in Dhofar 378. Their contents were obtained by SIMS and normalized with CI contents. Note that the REE patterns of the pyroxene cores are similar to those of the rims.

contents of high-Ca pyroxenes are higher by an order than those of low-Ca pyroxenes (Wadhwa *et al.*, 1994), pigeonitic pyroxenes #3 and #4 have lower REE contents than augitic pyroxenes #1 and #2, in spite of their occurrence that the former is rims and the latter is cores. The pyroxenes have no remarkable Eu anomalies, suggesting that the pyroxenes crystallized prior to or at the same time as plagioclases.

REE contents of the Dhofar 378 bulk rock were obtained by the INAA, and the CI-normalized REE pattern is shown to be flat and similar to Shergotty (Dreibus *et al.*, 2002). Comparing the bulk rock REE contents obtained by INAA with the pyroxene REE contents obtained by SIMS, the light REE are extremely depleted for the pyroxene data. The flat REE pattern of the INAA bulk rock may be explained by a suitable mixture of the REE-carrier phases such as Ca-phosphates, pyroxenes, and Pl-glass (Dreibus *et al.*, 2002).

6. Mineralogy

6.1. Clinopyroxenes

Clinopyroxenes in Dhofar 378 except Ti-rich augites and hedenbergite sometimes show mosaic extinction under a microscope, indicating that they experienced intense impact effects. The clinopyroxenes are augite, subcalcic augite, and pigeonite (Fig. 4), and the chemical compositions of pyroxenes are shown in Table 4. The mg# of clinopyroxenes range from 0.6 to less than 0.1 (Fig. 5). They zone from magnesian core to ferroan rims, and may reflect zonal patterns of the original lithology before the intense impact. Subcalcic clinopyroxene grains often show an exsolution texture, consisting of augite and pigeonite lamellae, and the width of the lamellae ranges from less than 1 μm

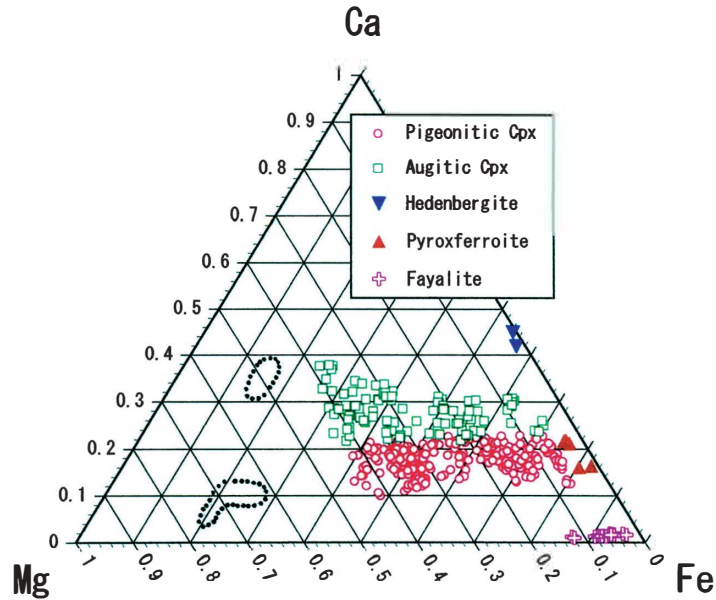


Fig. 4. Clinopyroxene (augite and pigeonite), hedenbergite, pyroxferroite, and fayalite in Dhofar 378 are shown in Ca-Mg-Fe atomic ratios. Clinopyroxenes with CaO more than 10 wt% and less than 10 wt% are conveniently taken to be augite and pigeonite, respectively. The compositional ranges of low-Ca and high-Ca pyroxenes in the ALHA77005 therszolithic shergottite (Ikeda, 1994) are shown for reference.

Table 4. Chemical compositions of pyroxenes and pyroxferroite in Dhofar 378. Columns [5] and [6] coexist.

	[1]	[2]	[3]	[4]	[5]	[6]	[7]	[8]
	m.Aug	f.Aug	m.Pig	f.Pig	lam.Aug	lam.Pig	Heden	Pyrox
SiO ₂	52.19	48.20	50.55	46.94	48.68	48.65	45.47	43.68
TiO ₂	0.21	0.43	0.21	0.23	0.43	0.40	2.60	1.11
Al ₂ O ₃	1.04	0.66	0.74	0.39	0.72	0.59	3.91	1.90
Cr ₂ O ₃	0.33	0.00	0.00	0.00	0.00	0.00	0.00	0.00
FeO	14.13	35.05	26.74	40.19	28.04	34.75	29.73	43.61
MnO	0.34	0.77	0.43	1.32	0.81	0.88	0.65	0.97
MgO	13.24	4.39	14.76	5.10	6.77	7.60	0.48	0.53
CaO	17.66	10.50	6.96	5.73	14.10	6.95	17.23	7.49
Na ₂ O	0.19	0.10	0.04	0.10	0.18	0.11	0.28	0.05
K ₂ O	0.00	0.00	0.04	0.01	0.05	0.00	0.00	0.00
Total	99.33	100.10	100.47	100.01	99.78	99.93	100.35	99.34
mg#	0.63	0.18	0.50	0.19	0.30	0.29	0.03	0.02

Abbreviation: magnesian(m.), ferroan(f.), lamellae(lam.), augite(Aug), pigeonite(Pig), hedenbergite(Heden), and pyroxferroite(Pyrox).

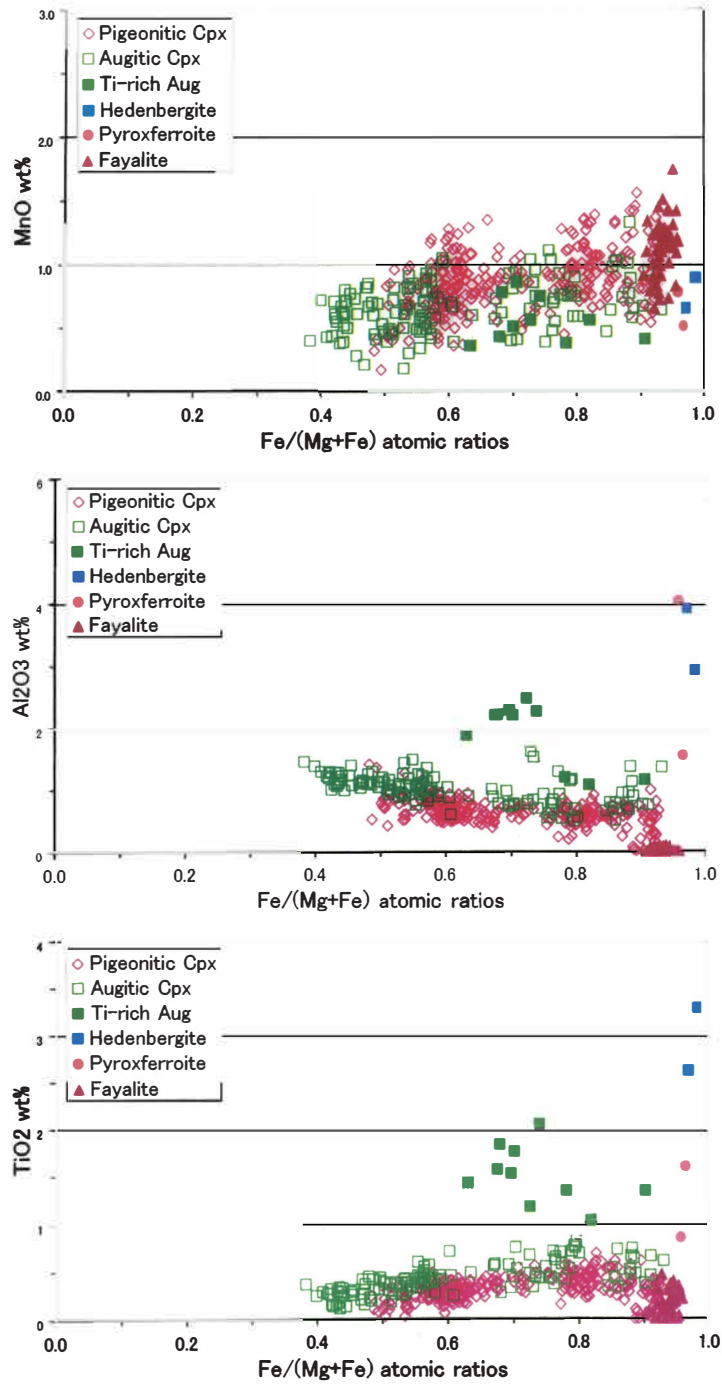


Fig. 5. Minor element contents (MnO, Al₂O₃, and TiO₂) of clinopyroxene (pigeonite and augite), Ti-rich augite with TiO₂ > 1 wt%, hedenbergite, pyroxferroite, and fayalite in Dhofar 378.

up to several μm (Fig. 2b). The MnO/FeO weight ratios of pyroxenes in Dhofar 378 are similar to those of other shergottites with the ratio of about 1.2/40 (McSween *et al.*, 1979).

Ti-rich augites have high TiO_2 contents more than 1 wt% (Fig. 5) and occur as small grains in mesostasis or between large magnesian pyroxene and/or Pl-glass grains (Fig. 2i). They are ferroan with $\text{mg}\# < 0.4$, and sometimes enriched in Al_2O_3 (Fig. 5). They are free from impact shock effects, suggesting that they have crystallized from impact melts. Hedenbergite occurs as euhedral crystals of lath shapes with several micron widths in fayalite-augite-plagioclase aggregates. The $\text{mg}\#$ ratios of hedenbergite are from 0.03 to 0.01. Hedenbergite never shows mosaic extinction and is free from the intense impact shock, suggesting its crystallization from impact melts.

6.2. Pl-glass and plagioclase rim

The main plagioclase component in Dhofar 378 is Pl-glass and not maskelynite, where the Pl-glass is a quenched melt having plagioclase compositions. The Raman spectra confirmed it (Dreibus *et al.*, 2002). All plagioclase grains in the original lithology of Dhofar 378 were melted by an intense impact shock. The Pl-glass has a stoichiometric compositions of plagioclase (Table 5) in spite of the intense impact shock. The Pl-glass has a cryptocrystalline plagioclase rim, which consists mainly of fibrous plagioclase (Fig. 2c). The fibrous plagioclase seems to have grown under a rapid cooling condition from the boundaries with pyroxene grains toward the cores of Pl-glass, and Becke's lines are observed at the boundaries between the glass core and the cryptocrystalline rim under a microscope (Fig. 2d). The width of the plagioclase rims range from a few tens of μm up to one hundred μm (Fig. 2e), and these rims completely surround the Pl-glass cores. Anorthite (An) mole contents of the plagioclase rims and Pl-glass cores are An_{40-56} and An_{33-50} , respectively (Table 5, Fig. 6). The plagioclase rims overlap in An contents to the Pl-glass cores, although the former are slightly more calcic than the latter. The orthoclase (Or) contents of the former ($\text{Or}_{<1.7}$) are lower than the latter ($\text{Or}_{1.7-12}$) (Fig. 6). The plagioclase rim consists of inner and outer rims (Fig. 2e). The outer rim is about $10\mu\text{m}$ wide and consists of clinopyroxene-plagioclase (Cpx-Pl) intergrowth, where needle crystals of clinopyroxene grows from the bounded clinopyroxene grains. The intergrown plagioclase of the outer rims is enriched in FeO contents (Fig. 7). At boundaries between clinopyroxene grains and plagioclase melts, Cpx-Pl melts may have been produced, and the melts crystallized clinopyroxene and Fe-bearing plagioclase to form the outer rims. After the precipitation of the outer rims, the plagioclase melts crystallized fibrous plagioclase under a rapid cooling condition to form the inner rims. Finally plagioclase melts quenched as Pl-glass in the cores. The inner rims are depleted in K_2O , and the Pl-glass is enriched in K_2O (Fig. 7). Figure 8 is a traverse of a plagioclase rim shown in Fig. 2e, which is perpendicular to the boundary of the plagioclase rim and clinopyroxene grains. The Pl-glass and plagioclase rims show slight chemical zoning. The inner rim is poor in K_2O and rich in An mole %, and the Pl-glass just in contact with the inner rim is enriched in K_2O and poor in An mole% (Fig. 8).

Fe-K-rich glass occurs as irregular small patches in plagioclase rims surrounding Pl-glass cores (Fig. 2f), and the chemical composition is shown in Table 5 (column 16).

Table 5. Chemical compositions of plagioclase (Pl), Pl-glass (gl), titanomagnetite (Mt), ilmenite (Ilm), silica (Si), whitlockite (Whitl), rhyolitic (Rhy.) glass, alkali feldspar (Fd), fayalite (Fa), and K-Fe-rich glass (K-Fe-gl), in Dhofar 378. The coexisting phases are [4]-[5], [6]-[7], and [10]-[11]-[12]-[13]-[14].

	[1]	[2]	[3]	[4]	[5]	[6]	[7]	[8]	[9]	[10]	[11]	[12]	[13]	[14]	[15]	[16]
	Pl-gl	front-gl	rim-Pl	Mt	Ilm	Si-gl	Quartz	Whitl	Apatite	Rhy.gl	ne.Fd	ne.Pl	q.Aug	milky gl	Fa	K-Fe-gl
SiO ₂	56.95	57.25	57.23	0.00	0.00	95.86	97.96	0.17	0.75	76.33	58.75	57.29	51.19	66.95	32.21	53.17
TiO ₂	0.00	0.02	0.00	25.34	50.80	0.18	0.09	0.00	0.00	1.07	0.13	0.02	0.15	1.21	0.00	0.04
Al ₂ O ₃	26.55	26.48	26.69	1.64	0.00	2.90	0.87	0.00	0.00	11.94	24.43	26.55	1.14	10.56	0.09	22.92
Cr ₂ O ₃	0.00	0.00	0.00	0.00	0.00	0.04	0.00	0.00	0.00	0.02	0.00	0.00	0.00	0.00	0.00	0.00
FeO	0.47	0.66	0.30	71.69	48.48	0.45	0.65	5.28	1.01	0.95	0.88	0.64	21.59	10.31	61.43	14.17
MnO	0.17	0.27	0.27	0.50	0.56	0.00	0.00	0.23	0.20	0.00	0.12	0.00	0.85	0.18	1.58	0.39
MgO	0.02	0.05	0.10	0.35	0.48	0.01	0.00	0.98	0.00	0.00	0.00	0.01	13.46	0.44	4.69	0.65
CaO	9.43	8.93	9.78	0.00	0.01	0.17	0.02	44.75	51.86	2.59	6.18	9.48	11.56	4.73	0.57	0.11
Na ₂ O	5.76	5.81	5.83	0.00	0.02	0.84	0.01	0.38	0.22	2.93	5.43	6.34	0.09	2.75	0.20	2.27
K ₂ O	0.24	0.67	0.15	0.00	0.04	0.03	0.00	0.00	0.00	3.48	3.65	0.30	0.06	2.05	0.00	4.72
P ₂ O ₅								45.56	42.53							
Total	99.59	100.14	100.35	99.52	100.39	100.48	99.60	97.35	*99.93	99.31	99.57	100.63	100.09	99.18	100.77	98.44
mg#										0.00				0.07	0.12	0.10

*: 2.16 wt% of Cl and 1.20 wt% of F are included, and the corresponding O should be subtracted. Abbreviation; front glass just in contact with Pl-rims(front-gl), needle-like(ne.), and quenched(q.).

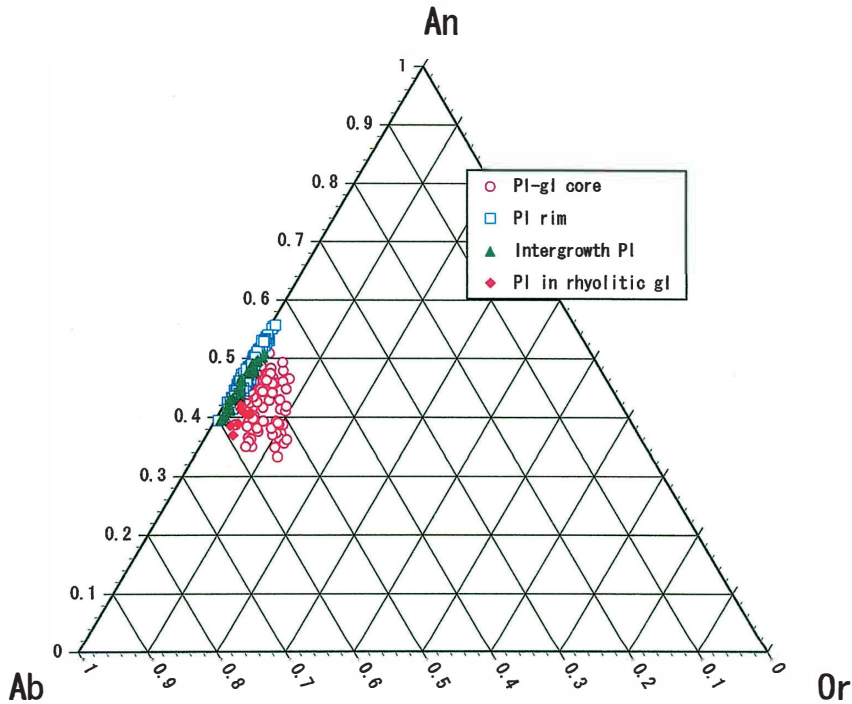


Fig. 6. The chemical compositions of plagioclase glass core (Pl-gl core), plagioclase rim (Pl rim), plagioclase (Pl) in intergrowths of clinopyroxene and plagioclase, needle-like plagioclase in rhyolitic glass (Pl in rhyolitic gl) in Dhofar 378 are shown in Ca(An)-Na(Ab)-K(Or) atomic ratios.

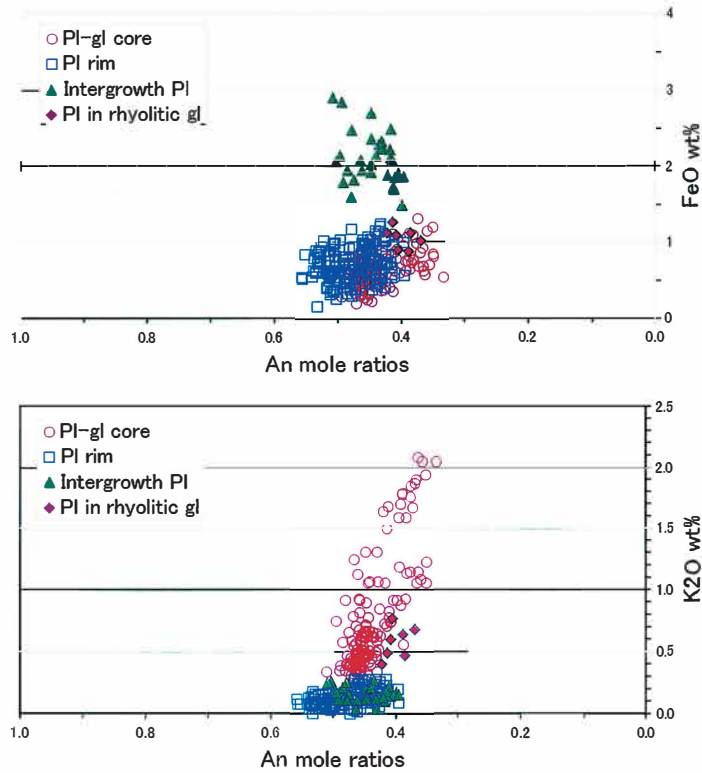


Fig. 7. FeO and K₂O contents of plagioclases and plagioclase-glass in Dhofar 378. The legend is the same as Fig. 6.

It seems to represent the residual melts that are locally and effectively piled up by crystallization of the plagioclase rims.

6.3. Mesostasis

Mesostasis in the original lithology was probably melted by an intense impact shock, and the mesostasis melts may have crystallized needle-like alkali feldspar (Fig. 2g). The residual melts may have resulted in rhyolitic glass (Fig. 2g), eutectic intergrowth of silicate and alkali feldspar, and milky glass (Fig. 2h). The milky glass is defined to be whitish glassy materials in back-scattered electron images (Fig. 2h).

The chemical compositions of the rhyolitic glass (column 10 in Table 5), milky glass (column 14), and alkali feldspar (column 11) in the mesostases are plotted with reference of the fusion-crust glass in Figs. 9 and 10. The rhyolitic glass is enriched in Na₂O and K₂O, and the Na/(Na + K) atomic ratios are about 0.5. The milky glass also has the ratios of about 0.5, but is enriched in CaO (Fig. 9), probably it may be a mixture of the rhyolitic glass and submicroscopic pyroxene grains. The alkali feldspar is enriched in Na₂O, K₂O and CaO, and the compositions are unusual in comparison of terrestrial alkali feldspars. Figure 9b shows that the unusual alkali feldspar was

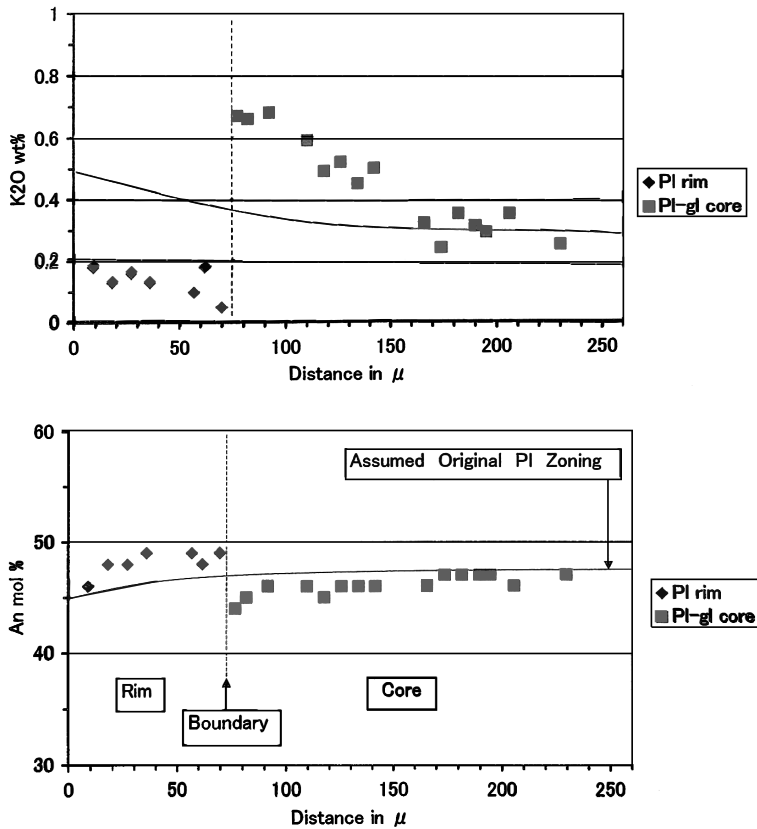


Fig. 8. Zoning profile of plagioclase rim and plagioclase-glass core in Dhofar 378. The horizontal axis is distance from a boundary with a pyroxene grain. The PI rim is lower in K_2O contents and higher in anorthite contents than the PI-glass core. The boundary between the rim and core is shown by a dash line. Note that the front glass just in contact with the boundary is enriched in K_2O by the pile-up effects in comparison to the PI-glass central core. Assumed original plagioclase zoning pattern are shown by solid lines.

produced at high temperatures around 1100°C .

6.4. Silica minerals

Silica minerals in the original lithology of Dhofar 378 occurred in mesostases and were melted by an intense impact, which produced silica minerals and silica glass in the mesostasis (Fig. 2j). Raman spectrum indicates that the silica minerals are mostly quartz (there is a peak of 465 cm^{-1}), associated with a minor amount of tridymite (peaks of 405 and 358 cm^{-1}). Their chemical compositions (Table 5) are plotted in Fig. 10. The silica glass is richer in alkalis, Al_2O_3 and FeO contents than the coexisting silica mineral.

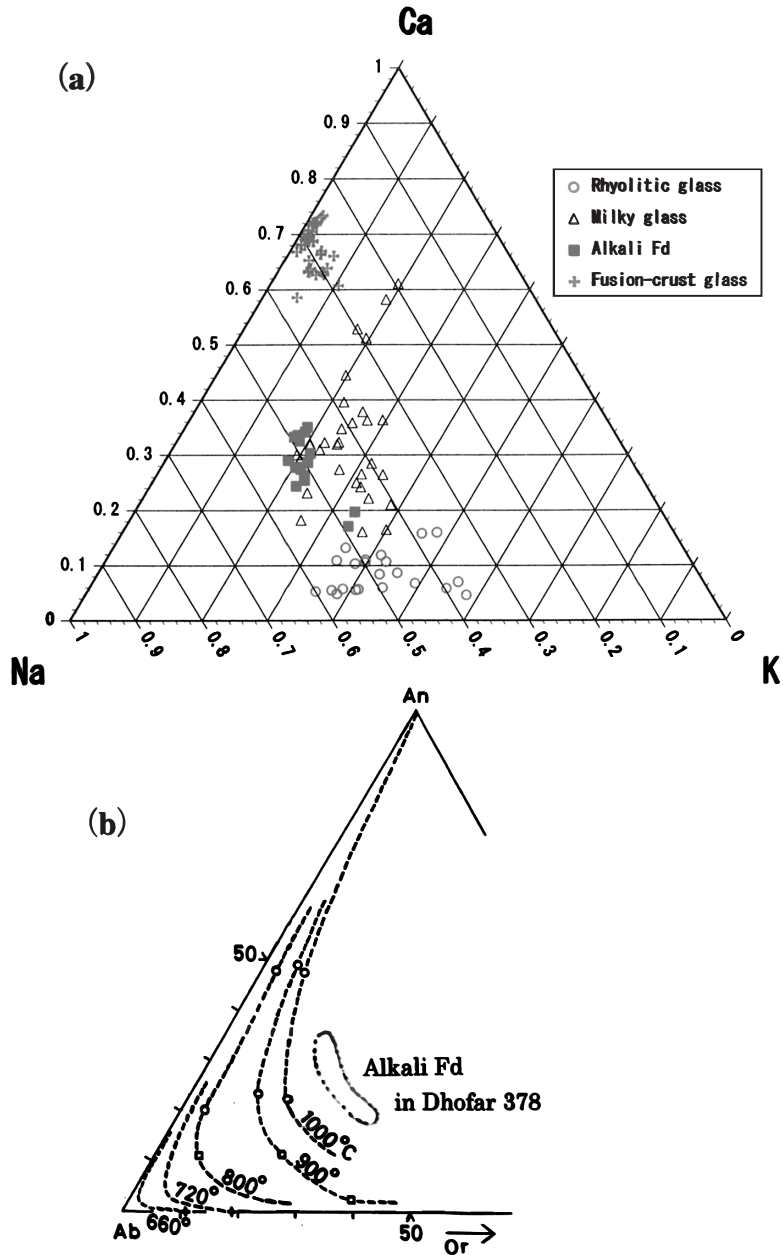


Fig. 9. (a) Ca-Na-K atomic ratios of rhyolitic glass, milky glass, and alkali feldspar in Dhofar 378. The fusion-crust glass is shown for reference. (b) Alkali feldspars in mesostasis of Dhofar 378 are shown by a dotted region. The isotherms of feldspar at temperatures of 660, 720, 800, 900 and 1000°C (Ikeda *et al.*, 1978) are shown by dashed lines for reference.

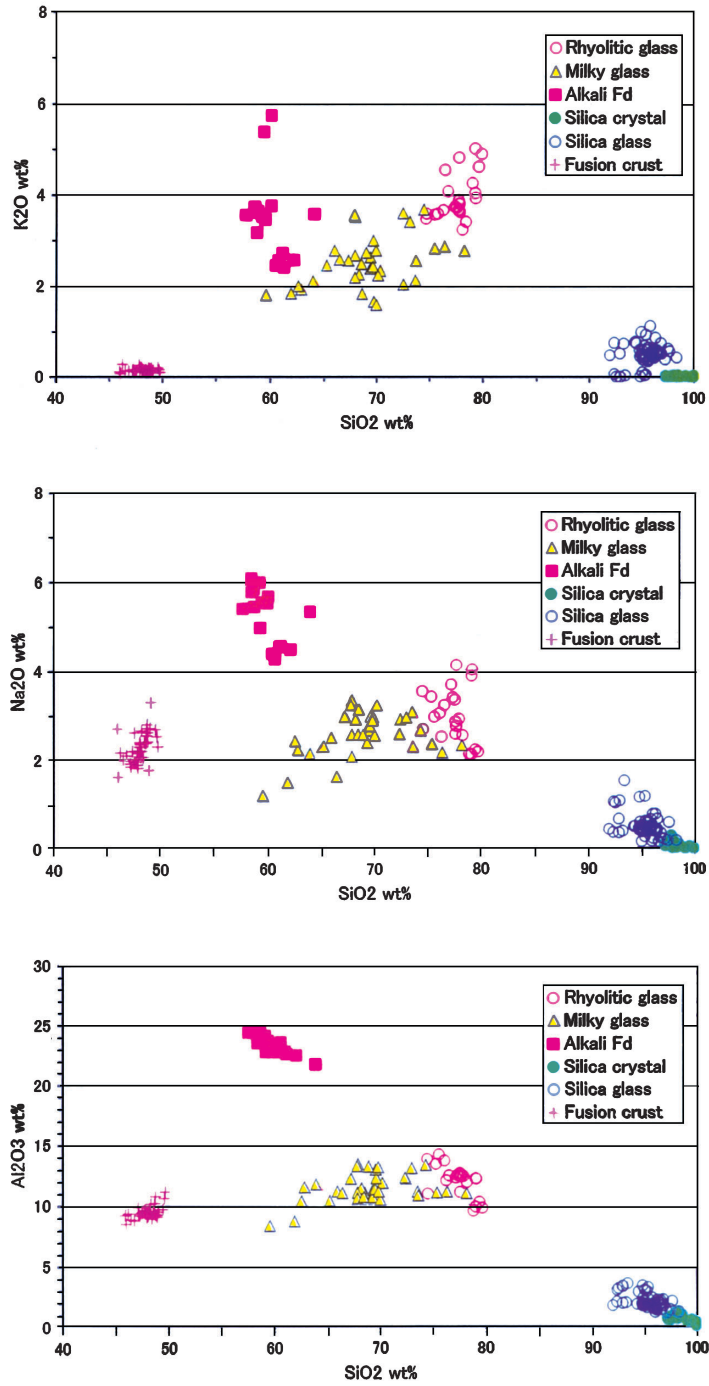


Fig. 10. The K₂O, Na₂O, and Al₂O₃ of glasses, alkali feldspar, and a silica mineral (quartz) in Dhofar 378. The glasses are rhyolitic, milky, and silica glass. The fusion-crust glass (Fusion crust) is shown for reference.

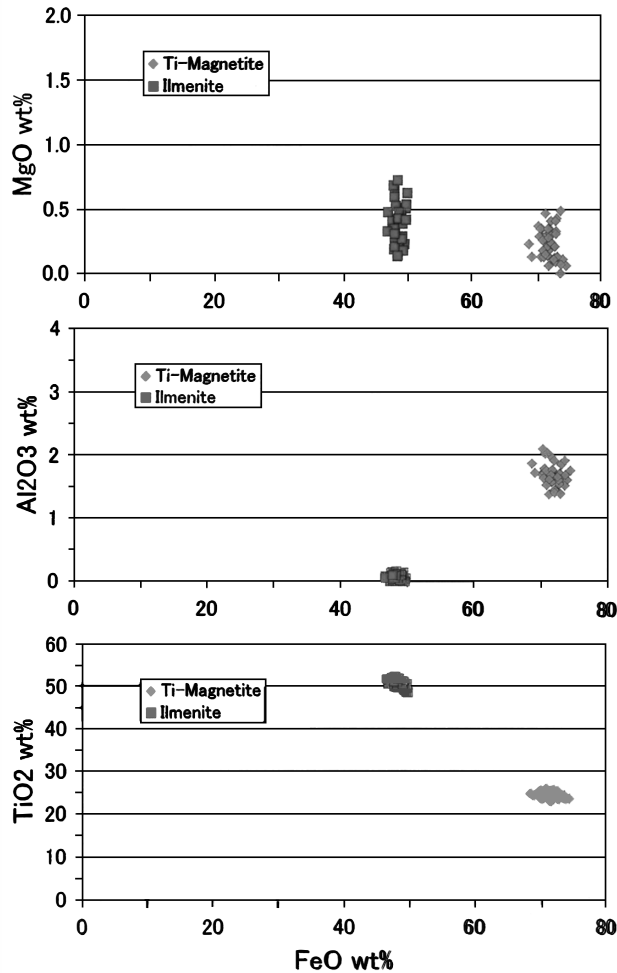


Fig. 11. The MgO, Al₂O₃, and TiO₂ contents of titanomagnetite (Ti-Magnetite) and ilmenite in Dhofar 378.

6.5. Magnetite and ilmenite

Titanomagnetite in Dhofar 378 includes ilmenite lamellae, a few tens of μm wide, which exsolved out from the host titanomagnetite (Fig. 21). Their chemical compositions are shown in Table 5 (columns 4 and 5). The titanomagnetite is enriched in TiO₂ (23–26 wt%) (Fig. 11), although their Al₂O₃ contents are low with 1.5–2.0 wt%. The average Ti/(Ti + Fe) atomic ratios of the host magnetite and lamellae ilmenite are 0.23 and 0.48, respectively.

6.6. Ca-phosphates

Phosphates in Dhofar 378 are mainly whitlockite with minor apatite, and their compositions are shown in Table 5 (columns 8 and 9). Whitlockite is identified by

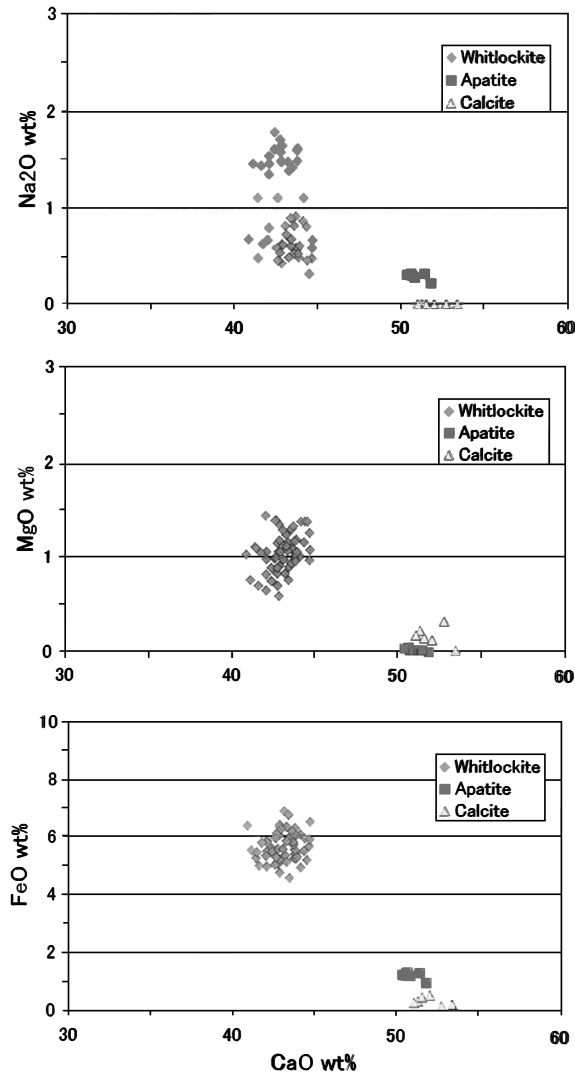


Fig. 12. The Na_2O , MgO , and FeO contents of whitlockite, apatite, and calcite. The calcite is a terrestrial alteration product.

Raman peaks ($970, 954, 606, 549, 442$ and 405 cm^{-1}), and any other phases are not identified in the whitlockite grains. Whitlockite often occurs as large grains up to a few hundred μm across and contains 5–6.5 wt% of FeO and 0.5–1.5 wt% of MgO (Fig. 12). The Na_2O contents vary from 0.3 to 1.8 wt%. The FeO , MgO and Na_2O contents of apatite are low in comparison to whitlockite. Chlorine and fluorine contents of apatite are 1.9–2.7 wt% and 1.2–1.5 wt%, respectively. There are magmatic inclusions in whitlockite, consisting of dacitic glass with minor pyroxferroite grains.

6.7. Olivine

Fayalite often occurs as intergrowth of fayalite and silica with minor clinopyroxene (Fig. 2k), as independent small fayalite grains (Fig. 2m), or as rims surrounding magnetite grains (Fig. 2n). The mg# ratios of fayalite range from 0.13 to 0.03 (Table 5, Fig. 4). The MnO contents are high with the range from 0.5–1.5 wt% (Fig. 5). The small fayalite grains and the rim fayalite around magnetite are free from any shock effects, indicating that they formed after an intense shock. They never associate with silica minerals and may have been produced mainly from magnetite by reaction with rhyolitic melts. On the other hand, intergrowths of fayalite and silica with minor clinopyroxene, several tens of microns across, may be a decomposition product of original pyroxferroite occurring before the impact shock.

6.8. Pyroxferroite

Small pyroxferroite, about 10 μm across, is free from shock effects and may have precipitated on pyroxene grains after the shock events (Fig. 2i). The pyroxferroite was identified using Raman spectroscopy (peaks of 991, 654, 381 and 307 cm^{-1}), in comparison with a synthetic pyroxferroite (peaks of 992, 658, 384 and 307 cm^{-1}). It is ferroan with mg#=0.02–0.03 (Table 4, column 8; Fig. 5), and the Al_2O_3 and TiO_2 contents are moderately high (Fig. 5). The small pyroxferroite may have crystallized together with Ti-rich augites and hedenbergite from impact melts.

Pyroxferroite occurs in some other shergottites. In QUE 94201, pigeonite cores are surrounded by an augite mantle, and they are further surrounded by ferroan pigeonite, hedenbergite, pyroxferroite (McSween *et al.*, 1996), where the pyroxferroite may be a primary mineral. The Los Angeles shergottite contains a fine-grained vermicular to micro-granulitic intergrowth of fayalite, hedenbergite and silica, and it is presumed to be a breakdown product of pyroxferroite (Rubin *et al.*, 2000). In addition to the intergrowth, an extremely ferroan phase, which is a pyroxferroite-like mineral, occurs as a rim on ferroan pigeonite in the Los Angeles meteorite (Mikouchi, 2001). The pyroxferroite-like mineral coexists with the decomposition product of pyroxferroite in the Los Angeles shergottite, and this situation is similar to those in the Dhofar 378 shergottite.

7. Discussion

7.1. Crystallization

Before the intense impact shock, Dhofar 378 was a doleritic rock showing an ophitic to subophitic texture, and it consisted mainly of plagioclase and pyroxenes with minor mesostasis. The parental melt crystallized pyroxene and plagioclase to form the ophitic texture. Finally the residual melt crystallized a silica mineral, alkali feldspar, ferroan pyroxene, pyroxferroite, and phosphates to form the mesostasis.

The pyroxenes in Dhofar 378 often show an exsolution lamellae texture. The lamellae are augite in pigeonite or vice versa, and seem to have been disturbed by an intense shock effect (Fig. 2b), indicating that they were produced prior to the intense shock event. Probably the formation of exsolution lamellae in subcalcic pyroxenes may have taken place at magmatic to subsolidus temperatures, and the Dhofar 378 may have

cooled slowly enough to form the exsolution lamellae after the crystallization of the subcalcic pyroxenes. The slow cooling may have resulted in decomposition of large pyroxferroite grains into fayalite-silica aggregates with minor clinopyroxene (Fig. 2k). Titanomagnetite also exsolved ilmenite lamellae (Fig. 2l) at subsolidus conditions.

7.2. Oxygen fugacity

Titanomagnetites in Dhofar 378 always contain exsolution lamellae of ilmenite. The averaged Ti/(Ti+Fe) atomic ratios of the host titanomagnetite and the exsolved ilmenite are 0.23 and 0.48, respectively (Table 5). On an assumption that the chemical compositions of the host titanomagnetite and lamellae ilmenite are stoichiometric and presented by [magnetite (Fe₃O₄) + ulvöspinel (Fe₂TiO₄)] and [ilmenite (FeTiO₃) + hematite (Fe₂O₃)], respectively, the FeO-Fe₂O₃-TiO₂ system (Buddington and Lindsley, 1964) gives the coexisting pair of titanomagnetite and ilmenite a temperature of about 900°C and an oxygen fugacity of 10⁻¹⁴ atmosphere. The oxygen fugacity is consistent with the QFM (quartz, fayalite, and magnetite) buffer and comparable to those of olivine-phyric shergottites (Herd, 2003).

7.3. FeO-rich whitlockite

Whitlockite in Dhofar 378 is enriched in FeO components up to 7 wt%, whereas coexisting apatite is not so rich in FeO with about 1.5 wt% FeO (Fig. 12). Although whitlockites in lherzolithic shergottites contain about 2.5–3.5 wt% MgO, 0.5–1.5 wt% FeO and 0.5–1.5 wt% Na₂O (Ikeda, 1994), some basaltic shergottites such as Zagami and Shergotty are high in FeO up to 4.4 wt% (McCoy *et al.*, 1992; Smith and Hervig, 1979). The whitlockite in Dhofar 378 contains about 0.5–1.5 wt% MgO, 5–7 wt% FeO, and 0.5–2.0 wt% Na₂O. The NWA 480 basaltic shergottite also contains FeO-rich whitlockite with about 5 wt% FeO (Grossman, 2001). The Los Angeles basaltic shergottite also contains FeO-rich whitlockite with about 5 wt% FeO, 1 wt% MgO, and 1 wt% Na₂O (Mikouchi, 2001; Warren *et al.*, 2004). Melt pockets in Zagami also contain FeO-rich whitlockite with 2.6–5.2 wt% FeO, and the MgO contents with 2.0–0.6 wt% is reversely correlated with the FeO content, suggesting the high FeO contents seems to be caused by fractional crystallization of FeO-enriched residual magma (McCoy *et al.*, 1999).

The chemical composition of the whitlockite in Dhofar 378 is homogeneous, and the high FeO contents of whitlockite could be caused by submicroscopic magnetite grains which would scatter homogenously in the whitlockite. However, Raman spectrum indicates that there are no other phases in whitlockite. In comparison with the normal whitlockites, MgO is depleted by about 2 wt%, and the depletion of MgO can be compensated by addition of 4 wt% FeO. Therefore, it is likely that the 5–6 wt% FeO resides in crystallographic lattice position site in the whitlockite structure, and the FeO-rich whitlockite may have precipitated from the FeO-enriched residual melt.

7.4. Impact shock

Dhofar 378 experienced intense impact shock, leaving the shock effects more or less on the all primary minerals which have originally crystallized from a Dhofar 378 magma. Pyroxene grains in Dhofar 378 sometimes show a mosaic extinction, planar

texture, mechanical twin, and mottled surface under a microscope. Sometimes pyroxene grains contain shock melt veins which consist mainly of needle-like pyroxenes (Fig. 2o). On the other hand, plagioclase, a silica mineral and the mesostasis were melted by the impact. They partially crystallized minerals, and residual melts quenched as glass under a rapid cooling condition.

The impact shock for Dhofar 378 is very intense in comparison to other shergottites, which contain maskelynite and are considered to be affected by a shock up to 45 GPa (Stöffler, 2000). The ALHA77005 lherzolitic shergottite contains Pl-glass instead of maskelynite, and the Pl-glass is often surrounded by thin plagioclase rims, suggesting the intense impact shock up to more than 45 GPa (Ikeda, 1994). The shock effects on Dhofar 378 is similar to that on ALHA77005, but all plagioclase grains in Dhofar 378 completely melted. In addition, the plagioclase rim is wider for the former (50–100 μm) than the latter (a few tens of μm). Shock melt pockets are not so developed in Dhofar 378 in comparison with ALHA77005, and this may be because plagioclase melt was more abundant for Dhofar 378 than ALHA77005. Flow structure is more remarkable for Dhofar 378 than for ALHA77005. The shock effects for Dhofar 378 seem to be more intense than ALHA77005. Dhofar 378 is intensely shocked to >45–55 GPa according to the calibration scheme of Stöffler *et al.* (1991) for ordinary chondrites (S6), and is higher than that of Los Angeles (<45–55 GPa). The shock pressure in Los Angeles is estimated to be 45 ± 3 GPa (Fritz *et al.*, 2005), and the whole rock melting takes place at pressures higher than 75 GPa (Stöffler *et al.*, 1991), suggesting that the shock degree for Dhofar 378 may be around 55–75 GPa.

7.5. Plagioclase rim

All primary plagioclase grains in Dhofar 378 were melted by an intense impact shock to produced plagioclase melt. In addition, a plagioclase-pyroxene melt was also produced between pyroxene grains and the plagioclase melt. The plagioclase-pyroxene melt was very thin, about ten micrometers wide, and crystallized under a rapid cooling condition to form the outer rim of Pl-glass (Fig. 2e). The intergrown plagioclase is rich in FeO (Fig. 7), because the plagioclase-pyroxene melt included abundant FeO. After the precipitation of the outer rim, fibrous plagioclase crystallized under a rapid cooling condition from the plagioclase melt to produce the inner rim (Fig. 2e). The boundary between the outer and inner rims is unclear, but the boundary between the inner rim and Pl-glass core is sharp.

The K_2O contents of the Pl-glass which contacts directly with the plagioclase rims tend to be higher than those of Pl-glass occurring far from the contact (Fig. 8). This suggests that the plagioclase melt crystallized fibrous plagioclase rims to pile up the K_2O content in the plagioclase melt just in front of the growing fibrous plagioclase rims.

7.6. Comparison to other shergottites

The Dhofar 378 basaltic shergottite is one of the most ferroan meteorites among all shergottites. It is very similar in bulk and mineral chemical composition and mineral assemblage and occurrence to those of the Los Angeles basaltic shergottite. However, the degree of the impact shock for Dhofar 378 differs from that of Los Angeles, and is the highest among all known martian meteorites, resulting in melting of all plagioclase

grains in the original lithology of Dhofar 378. The shock-induced temperature may be the highest among all known martian meteorites. Dhofar 378 was so disturbed by the intense impact shock that the internal crystallization ages of Rb-Sr for Dhofar 378 may not be obtained.

8. Conclusions

(1) Dhofar 378 is a basaltic shergottite, which shows the most ferroan lithology among the all known martian meteorites. Dhofar 378 resembles the Los Angeles basaltic shergottite in lithology and mineral chemistry, although the shock stage of Dhofar 378 is higher than that of the Los Angeles shergottite. The degree of impact shock for Dhofar 378 may be about 55–75 GPa and is the highest among all known martian meteorites.

(2) Clinopyroxene grains often contain exsolution lamellae, suggesting that the original lithology of Dhofar 378 was cooled slowly enough to precipitate the lamellae. This is consistent with the doleritic texture of Dhofar 378 with coarse-grained major phases (Cpx and Pl-gI).

(3) The oxygen fugacity of Dhofar 378 under a subsolidus condition was estimated by using titanomagnetite with lamellae ilmenite and is around the QFM buffer.

(4) All plagioclase grains in the original lithology were melted by an intense impact. The plagioclase melt crystallized fibrous plagioclase to form the rims, and finally the plagioclase melt quenched as Pl-glass to form the core in a rapid cooling condition.

(5) REE contents of augitic cores and pigeonitic rims for Dhofar 378 are similar to each other, and the REE patterns of pyroxenes resemble those for other shergottites.

Acknowledgments

We thank Dr. N. Nakamura for his discussion concerning on the chronological data of Dhofar 378.

References

- Bence, A.E. and Albee, A.L. (1968): Empirical correction factors for the electron microanalysis of silicates and oxides. *J. Geol.*, **76**, 382–403.
- Buddington, A.F. and Lindsley, D.H. (1964): Iron-titaniferrous oxide minerals and synthetic equivalents. *J. Petrol.*, **5**, 310–357.
- Dreibus, G., Wlotzka, F., Huisl, W., Jagoutz, A., Kubny, A. and Spettel, B. (2002): Chemistry and petrology of the most feldspathic shergottite: Dhofar 378. *Meteorit. Planet. Sci.*, **84** (Suppl), A201.
- Fritz, J., Artemieva, N. and Greshake, A. (2005): Ejection of Martian meteorites. *Meteorit. Planet. Sci.*, **40**, 1393–1411.
- Grossman, J.N. (2001): The Meteoritical Bull., No. 85. *Meteorit. Planet. Sci.*, **36**, A293.
- Herd, C.D. (2003): The oxygen fugacity of Ol-phyric martian basalts and the components within the mantle and crust of Mars. *Meteorit. Planet. Sci.*, **38**, 1793–1805.
- Ikeda, Y. (1994): Petrography and petrology of the ALH-77005 shergottite. *Proc. NIPR Symp. Antarct. Meteorites*, **7**, 9–29.
- Ikeda, Y. (2004): Petrology of the Y980459 glassy basaltic shergottite. *Antarct. Meteorite Res.*, **17**, 35–54.

- Ikeda, Y., Tagiri, M. and Takahashi, M. (1978): Geothermometer by the solubility of an orthoclase component in plagioclase. *Zôgan-Kôbutsu Sôgô-Kenkyu*, at 1978 supported by the grant of the Monbusho (Japanese Ministry of Education, Sport and Culture) (in Japanese).
- Kita, N.T., Ikeda, Y., Togashi, S., Liu, Y.Z., Morishita, Y. and Weisberg, M.K. (2004): Origin of ureilites inferred from a SIMS oxygen isotopic and trace element study of clasts in the Dar al Gani 319 polymict ureilite. *Geochim. Cosmochim. Acta*, **68**, 4213–4235.
- Lundberg, L., Crozaz, G., McKay, G. and Zinner, E. (1988): Rare earth element carriers in the Shergotty meteorite and implications for its chronology. *Geochim. Cosmochim. Acta*, **52**, 2147–2163.
- McCoy, T.J., Wadhwa, M. and Keil, K. (1999): New lithologies in the Zagami meteorite: evidence from fractional crystallization of a single magma unit on Mars. *Geochim. Cosmochim. Acta*, **63**, 1249–1262.
- Mikouchi, T. (2001): Mineralogical similarities and differences between the Los Angeles basaltic shergottite and the Asuka-881757 lunar mare meteorite. *Antarct. Meteorite Res.*, **14**, 1–20.
- McSween, H.Y., Stolper, E.M., Taylor, L.A., Muntean, R.A., O’Kelley, G.D., Eldridge, J.S., Biswas, S., Ngo, H.T. and Lipschutz, M.E. (1979): Petrogenetic relationship between Allan Hills 77005 and other Achondrites. *Earth Planet. Sci. Lett.*, **45**, 275–284.
- McSween, H.Y., Eisenhour, D.D., Taylor, L.A., Wadhwa, M. and Crozaz, G. (1996): QUE 94201 shergottite: Crystallization of a martian basaltic magma. *Geochim. Cosmochim. Acta*, **60**, 4563–4569.
- Rubin, A.E., Warren, P.H., Greenwood, J.P., Verish, R.S., Leshin, L.A. and Hervig, R.L. (2000): Petrology of Los Angeles: A new basaltic shergottite find. *Lunar and Planetary Science XXXI*. Houston, Lunar Planet. Inst., Abstract #1963 (CD-ROM).
- Russell, S.S., Zipfel, J., Grossman, J.N. and Grady, M.M. (2002): The Meteoritical Bulletin No.86. *Meteorit. Planet. Sci.*, **37**, A157–A184.
- Smith, J.V. and Hervig, R.L. (1979): Shergotty meteorite: mineralogy, petrography and minor elements. *Meteoritics*, **14**, 121–142.
- Stöfler, D. (2000): Maskelynite confirmed as diaplectic glass: Indication for peak shock pressures below 45 GPa in all Martian meteorites. *Lunar and Planetary Science XXXI*. Houston, Lunar Planet. Inst., Abstract #1170 (CD-ROM).
- Stöfler, D., Keil, K. and Scott, E.R.D. (1991): Shock metamorphism of ordinary chondrites. *Geochim. Cosmochim. Acta*, **55**, 3845–3867.
- Togashi, S., Kita, N.T., Tomiya, A., Morishita, Y. and Imae, N. (2003): Melt contribution to partitioning of trace elements between plagioclase and basaltic magma of Fuji volcano, Japan. *Appl. Surf. Sci.*, **203–204**, 814–817.
- Wadhwa, M., McSween, H. and Crozaz, G. (1994): Petrogenesis of shergottite meteorites inferred from minor and trace element microdistributions. *Geochim. Cosmochim. Acta*, **58**, 4213–4229.
- Warren, P.H., Greenwood, J.P., Richardson, J.W., Rubin, A.E. and Verish, R.S. (2000): Geochemistry of Los Angeles, a ferroan, La- and Th-rich basalt from Mars. *Lunar and Planetary Science XXXI*. Houston, Lunar Planet. Inst., Abstract #2001 (CD-ROM).
- Warren, P.H., Greenwood, J.P. and Rubin, A.E. (2004): Los Angeles: A tale of two stones. *Meteorit. Planet. Sci.*, **39**, 137–156.